*Carnegie Observatories Astrophysics Series, Vol. 1:*
*Coevolution of Black Holes and Galaxies, 2004*
*ed. L. C. Ho (Pasadena: Carnegie Observatories,*
*http://www.ociw.edu/ociw/symposia/series/symposium1/proceedings.html)*

# $z \sim 6$ Quasars in the Sloan Digital Sky Survey

X. FAN[1], M. A. STRAUSS[2], D. P. SCHNEIDER[2], R. H. BECKER[4],
R. L. WHITE[5], and L. PENTERRICCI[6]
*(1) University of Arizona, (2) Princeton University, (3) Pennsylvania State University,*
*(4) UC Davis and LLNL, (5) STScI, (6) MPIA*

**Abstract**

We present the recent results on a survey for quasars at $z \sim 6$, selected from $\sim 3000$ deg$^2$ of multicolor imaging data from the Sloan Digital Sky Survey (SDSS). Seven luminous ($M \sim -27$) quasars at $5.7 < z < 6.4$ are discovered. The existence of strong metal lines in the quasar spectra suggests early metal enrichment in the quasar environment. These quasars, if not gravitationally lensed, are located in supermassive black holes of $M \sim 10^{9-10} M_\odot$, indicating rapid formation of supermassive black hole population in the early universe, probably co-eval with the formation of the first generation galaxies. We find that at $z = 6$, the comoving density of luminous quasars declines by a factor of $\sim 20$ from $z \sim 3$. The strength of Ly$\alpha$ absorption increases strongly with redshift. In particular, Keck and VLT spectroscopy of the highest redshift quasars reveal the first detections of complete Gunn-Peterson troughs at $z \gtrsim 6$. By comparing with cosmological simulations, we find that the ionizing background declines by a factor of $> 20$ from $z \sim 3$ to 6, while the neutral faction increases by $> 100$. The ionization state of the IGM at $z \sim 6$ is typical of those in at the end of overlap stage of the reionization epoch. Thus, $z \sim 6$ markes the end of the cosmic dark ages.

## 1.1 Introduction

High-redshift quasars provide direct probes of the epoch when the first generation of galaxies and quasars formed. The existence of very luminous quasars at high redshift, likely residing in massive halos, constrains models of the formation of massive black holes and quasar evolution. The absorption spectra of high-redshift quasars reveal the state of the intergalactic medium and the evolution of the ionization background at early epochs. As shown in this proceeding (see also Fan et al. 2001b, 2002, 2003, Becker et al. 2001, Pentericci et al. 2002), the observations of the highest redshift quasars known today may finally constrain when the reionization happened, thus ended the cosmic dark ages, and how the universe was transformed from mostly neutral to mostly ionized by the light of first generation galaxies and quasars.

Sloan Digital Sky Survey (SDSS; York et al. 2000) uses a dedicated 2.5m telescope and a large format CCD camera (Gunn et al. 1998) at the Apache Point Observatory in New Mexico to obtain images in five broad bands ($u$, $g$, $r$, $i$ and $z$) over 10,000 deg$^2$ of high Galactic latitude sky. The goal of the SDSS quasar survey is to establish a color-selected, flux-limited sample of $\sim 10^5$ quasars over the entire survey area. Quasar candidates are selected based on their broad-band colors from the SDSS five color photometry (Fan et al.

1999, Richards et al. 2001). Over 200 quasars at $z > 3.5$ have been discovered to date from the SDSS multicolor imaging data (Anderson et al. 2001 and reference therein). The inclusion of the reddest band, $z$, in principle enables the discovery of quasars up to $z \sim 6.5$ from the SDSS data (Fan et al. 2000).

## 1.2 Discovery of $z \sim 6$ Quasars

We have carried out a systematic survey of $i$-dropout quasars ($z > 5.7$, whose Ly$\alpha$ forest is entirely in the $i$ band) based on the SDSS imaging data (Fan et al. 2001b). The observed colors of quasars evolve strongly with redshift, as the intrinsic emission and the intervening absorption spectral features move through the SDSS filter system. At $z > 5.7$, the Ly$\alpha$ emission line begins to move out of the SDSS $i$ filter. With an average $i^* - z^* > 2$, these high-redshift quasars have undetectable flux in the bluer $u$, $g$ and $r$ bands, and little flux (sometimes also undetectable) in $i$ band. They become $i$-dropout objects with only one measurable color in SDSS photometry.

Quasars at $z > 5.8$ are extremely rare on the sky. We found four $i$-dropout quasars in 1550 deg$^2$. For comparison, over the same area, there are about 15 million objects detected in the $z$ band above 6-$\sigma$, and about 6.5 million cosmic ray hits in the $z$ band. The quasars are faint, with low signal-to-noise ratio (S/N) photometry from the SDSS imaging data. Therefore, the key to a successful selection process is an efficient elimination of potential contaminants. We face three technical challenges:

(1) Elimination of false $z$-band only detections, composed primarily of cosmic rays, but also including satellite trails, electronic ghost images and bleed trails from bright stars. We have developed sensitive cosmic ray classification routine to reject these false detections.

(2) Reliability of $z^*$ photometry. Objects in the tail of the error distribution could scatter into the selected region of color space, and pose a serious contamination when a large number of objects is searched. We carry out an additional round of $z$ band photometry on the $i$-dropout objects using separated telescope to improve the photometric accuracy.

(3) Separating quasars and cool dwarfs. The surface density of cool dwarfs, with spectral types ranging from mid-L to T, which have $i^* - z^* > 2.2$ (Geballe et al. 2002, Leggett et al. 2002), is $\sim 15$ times higher than that of $z > 5.7$ quasars. We use $J$-band photometry to separate these two classes of objects.

We have discovered seven quasars at $z > 5.7$ in the 3000 deg$^2$ of the survey area in the redshift range between 5.7 and 6.4. Their spectra are presented in Figure 1.1. As a by-product of the survey, a large number of L dwarfs and a dozen T dwarfs are discovered. They form a complete sample of L and T dwarfs, enable study of the luminosity function and mass function of substellar objects (Knapp et al. 2004).

## 1.3 Quasar Evolution at $z \sim 6$

Emission line ratios can be used to measure the metallicity of the gas in the Broad Emission Line Region (BELR). There is growing evidence from those measurements that BELR have roughly solar or higher metallicities even out to $z > 4$ (Hamman & Ferland 1999). We use the spectra of our quasars to estimate the quasar metallicity at $z \sim 6$. Of various line ratios, the NV $\lambda$1240/CIV $\lambda$1549 ratio and NV $\lambda$1240/HeII $\lambda$1640 ratio are particularly useful abundance diagnostics (Hamman & Ferland 1993, 1999). The sensitivity of NV/CIV to metallicity is due to the fact that N is a secondary element, with abundance proportional to $Z^2$, while C is a primary element with abundance proportional to $Z$. Using

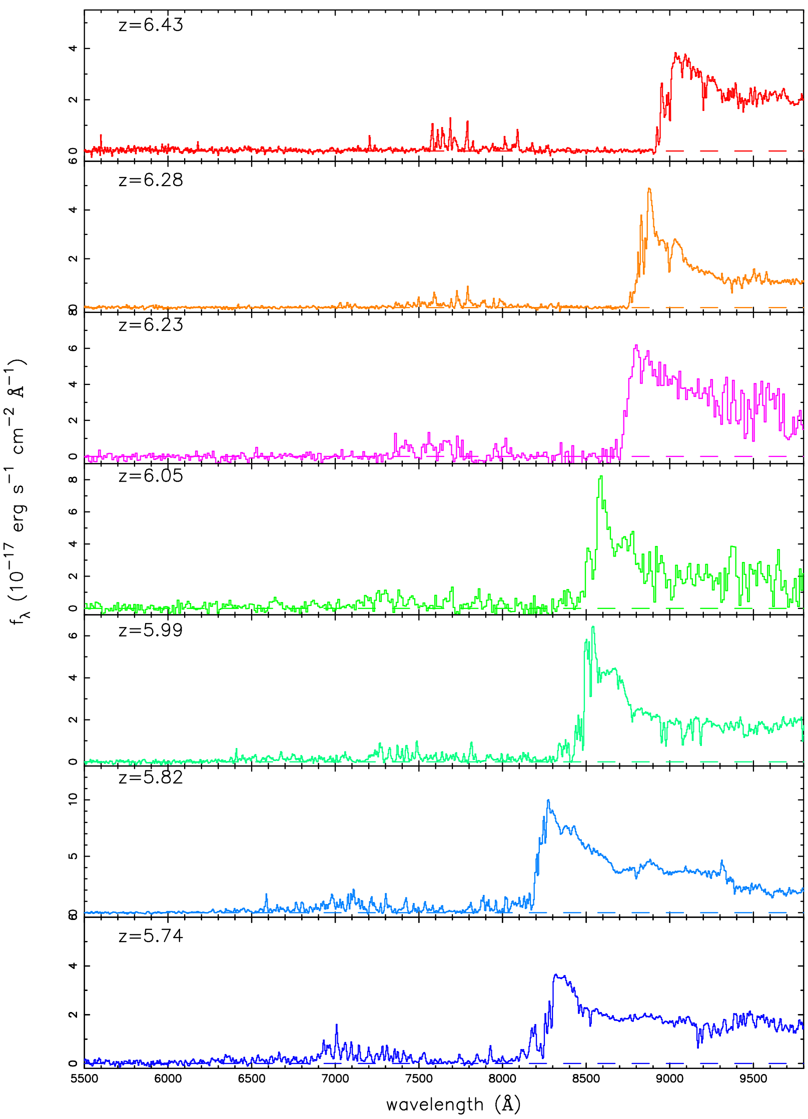


Fig. 1.1. Low resolution spectra of seven SDSS quasars at $z > 5.7$.

the optical/IR spectrum of SDSS 1030+0524 (Fan et al. 2001b, Becker et al. 2001), we find the flux ratios NV/CIV $\sim 0.7$ and NV/HeII $> 1.5$. Both values imply super-solar metallicity of the BELR region, suggesting rapid chemical enrichment and multiple generation of star formation in the quasar environment at these very early epochs.

Based on a sample of six quasars at $z > 5.7$ that cover 2870 deg$^2$ presented in Fan et al.

(2001) and Fan et al. (2003), we estimate the comoving density of luminous quasars at $z \sim 6$ and $M_{1450} < -26.8$ to be $(8 \pm 3) \times 10^{-10}$ Mpc$^{-3}$ (for $H_0$ = 50 km s$^{-1}$Mpc$^{-1}$, $\Omega$ = 1). HST imaging of two $z > 5.7$ quasars and high-resolution ground-based images (seeing $\sim 0.4''$) of three additional $z > 5.7$ quasars show that none of them is gravitationally lensed. The luminosity distribution of the high-redshfit quasar sample suggests the bright end slope of the quasar luminosity function at $z \sim 6$ is shallower than $\Psi \propto L^{-3.5}$ (2-$\sigma$), consistent with the absence of strongly lensed objects.

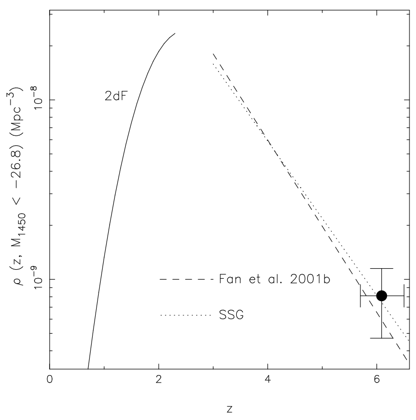


Fig. 1.2. The evolution of quasar comoving spatial density at $M_{1450} < -26.8$ in the $\Omega$ = 1 model (h=0.5). The large dot represents the result from this survey. The dashed and dotted lines are the best-fit models from Fan et al. (2001a) and Schmidt et al. (1995), respectively. The solid line is the best-fit model from the 2dF survey (Boyle et al. 2000) at $z < 2.5$.

Assuming that these luminous quasars are radiating at Eddington limit and they are magnified by gravitational lensing, if the relation between black hole mass and bulge mass observed at $z \sim 0$. these quasars are likely to reside in dark matter halos with $\sim 10^{13}$M$_\odot$, represent $\sim$ 5-$\sigma$ peaks in the density field and are located on the tail of the mass function at early epochs. The comparison between the slope of the quasar luminosity function and mass function at $z \sim 6$ will put strong constraints on models of quasar formation at early epochs. Models associating quasars with dark matter halos, such as the ones by Haiman & Loeb (1998), predict a steep halo mass function for these quasars ($\beta$ between –5 and –6 for the mass function).

The shape of the quasar luminosity function is also crucial in understanding the contribution of the quasar population to the UV ionizing background at high redshift. We calculated the total emissivity per unit volume of ionizing photons from the quasar population and compared it with what is required to keep the universe ionized. Figure 10 of Fan et al. (2001) indicates that with $\beta_l > -3.5$ and a range of assumptions about the characteristic luminosity and faint-end slope, quasars are not likely to produce enough photons to ionize the universe or to keep it ionized at $z \sim 6$, unless the luminosity function rises sharply at lower luminosities.

The current SDSS survey can only detect and select the most luminous $z \sim 6$ quasars with $M_{1450} \lesssim -26.5$. A deep quasar survey at $z \sim 6$ is needed to understand the complete picture of high-redshift quasar evolution and its relation to the reionization history. The SDSS Southern Survey covers a 200 deg$^2$ region about 1.5 – 2 mag deeper than the SDSS main sample. Assuming a quasar luminosity function of $\Psi \propto L^{-3}$, and the density of $z > 5.7$ quasars for $z^* < 20$ is 6 objects per 3000 deg$^2$, we expect to find 16 quasars at $z > 5.7$ and $z^* < 22$ in this 200 deg$^2$. By comparison, we expect to find $\sim 20$ quasars at $z > 5.7$ and $z^* < 20$ in the 10,000 deg$^2$ of main SDSS survey area.

## 1.4 Lyman Absorption and Complete Gunn-Peterson Troughs

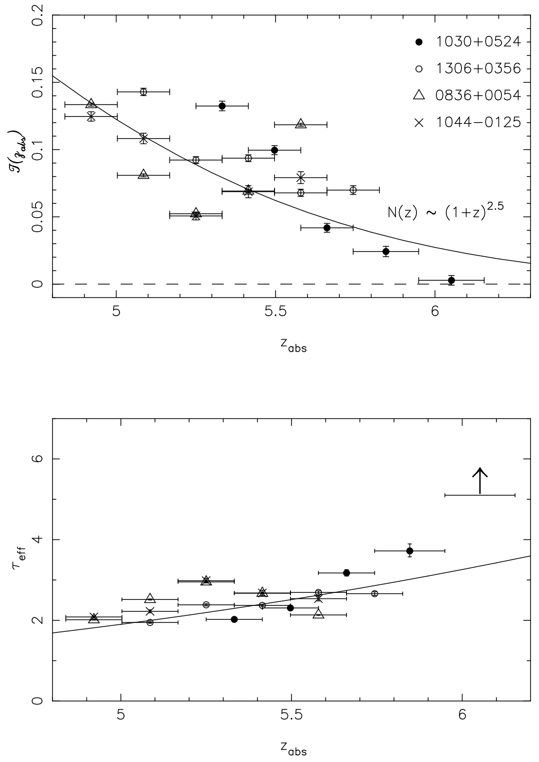


Fig. 1.3. Evolution of transmitted flux ratio and effective Gunn-Peterson optical depth as functions of redshift. The solid line is the expected evolution if the number density of Ly$\alpha$ clouds increases as $N(z) \propto (1+z)^{2.5}$. No flux is detected in the spectrum of SDSS 1030+0524 at $z_{abs} \sim 6$, indicating $\tau_{eff} > 5.0$.

We have obtained high S/N, moderate resolution spectroscopy of these $z > 5.7$ quasars using Keck (Fan et al. 2000, Becker et al. 2001, Fan et al. 2003) and VLT (Pentericci et al. 2002) telescopes to study the evolution of HI absorption at high-redshift. Figure 1.3 illustrate the evolution of transmitted flux and effective optical depth in the Ly$\alpha$ forest region along the four lines of sight. We find that the Ly$\alpha$ absorption in the spectra of these quasars evolves strongly with redshift. To $z \sim 5.7$, the Ly$\alpha$ absorption evolves as expected from an extrapolation from lower redshifts. However, in SDSS 1030+0524 ($z = 6.28$), the average transmitted flux is $0.0038 \pm 0.0026$ times that of the continuum level over 8450 Å $< \lambda <$ 8710Å ($5.95 < z_{abs} < 6.16$), consistent with zero flux. Thus the flux level drops by a factor of $> 150$, and is consistent with zero flux in the Ly$\alpha$ forest region immediately blueward of the Ly$\alpha$ emission line, compared with a drop by a factor of $\sim 10$ at $z_{abs} \sim 5.3$. A similar break is seen at Ly$\beta$; because of the decreased oscillator strength of this transition, this allows us to put a considerably stronger limit, $\tau_{eff} > 20$, on the optical depth to Ly$\alpha$ absorption at $z = 6$.

This is a clear detection of a complete Gunn-Peterson (1965) trough, caused by neutral hydrogen in the intergalactic medium. Even a small neutral hydrogen fraction in the intergalactic medium would result in an undetectable flux in the Ly$\alpha$ forest region. Therefore, the existence of the Gunn-Peterson trough by itself does not indicate that the quasar is observed prior to the reionization epoch. However, the fast evolution of the mean absorption in these high-redshift quasars suggests that the mean ionizing background along the line of sight to this quasar has declined significantly from $z \sim 5$ to 6, and the universe is approaching the reionization epoch at $z \sim 6$.

SDSS 1148+5251 ($z = 6.43$) is currently the highest redshift quasar known. Its spectrum also shows clear presence of a complete Gunn-Peterson (1965) trough from $\sim$ 8300Å to $\sim$ 8900Å imilar to the one detected in SDSS J1030+0524. Detailed analysis of the Gunn-Peterson trough in this object is currently underway, and it will provide us crucial information on he Gunn-Peterson effect along the different lines of sight, and place constraints on the nature of ionizing sources and the state of IGM at these critical redshifts.

## 1.5 Constraining the Epoch of Reionization

We study the process of cosmic reionization and estimate the ionizing background in the intergalactic medium (IGM) using the Lyman series absorption in the spectra of four quasars at $5.7 < z < 6.3$. Figure 1.4 illustrates the evolution of the ionization state of the IGM at high redshift inferred from observations. First, we derive the redshift evolution of the ionizing background at high redshifts, using both semi-analytic techniques and cosmological simulations to model the density fluctuations in the IGM. The existence of the complete Ly$\alpha$ Gunn-Peterson trough in the spectrum of the $z = 6.28$ quasar SDSS 1030+0524 indicates a photoionization rate ($\Gamma_{-12}$ in units of $10^{-12}\text{s}^{-1}$) at $z \sim 6$ lower than 0.08, at least a factor of 6 smaller than the value at $z \sim 3$. The Ly$\beta$ and Ly$\gamma$ Gunn-Peterson troughs give an even stronger limit $\Gamma_{-12} < 0.02$ due to their smaller oscillator strengths, indicating that the ionizing background in the IGM at $z \sim 6$ is more than 20 times lower than that at $z \sim 3$.

We also find that the volume-averaged neutral hydrogen fraction increases from $10^{-5}$ at $z \sim 3$ to $> 10^{-3}$ at $z \sim 6$. At this redshift, the mass-averaged neutral hydrogen fraction is larger than 1%; the mildly overdense regions ($\delta > 3$) are still mostly neutral and the comoving mean free path of ionizing photons is shorter than 8 Mpc. In Figure 1.4, we compare these values with the simulation of cosmological reionization by Gnedin (2000), which includes 3-D radiative transfer, star formation process and detailed atomic and molecular physics. We find that that the observed properties of the IGM at $z \sim 6$ are typical of those in the era at the end of the overlap stage of reionization when the individual HII regions merge. Thus, $z \sim 6$ marks the end of the reionization epoch. Even though the current observations certainly cannot probe deeper into the reionization epoch, the near phase-transition behavior of the ionization state of the IGM at $z \sim 6$, and the narrow redshift range over which this process occurs in cosmological reionization simulations both imply that the reionization redshift *cannot be at a redshift much higher than six*.

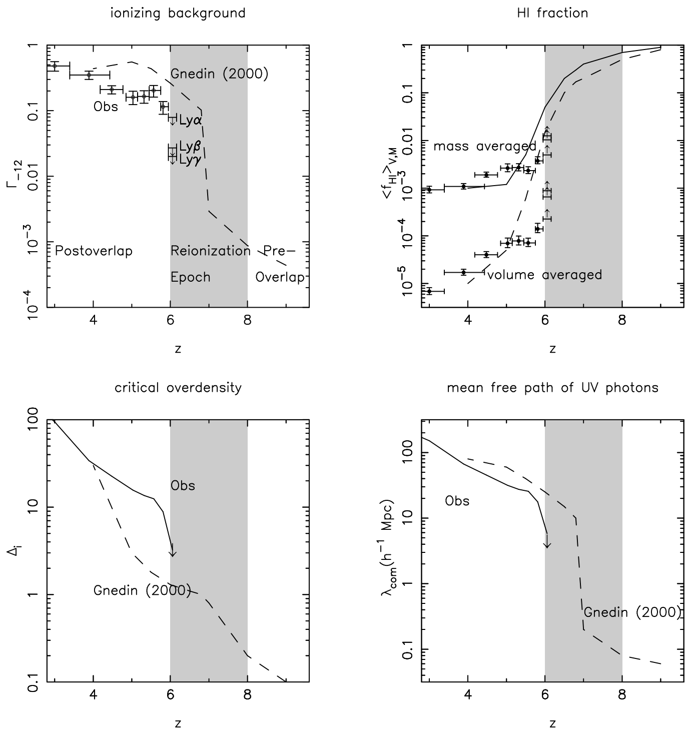


Fig. 1.4. Evolution of the ionization state of the IGM inferred from the observations. It is compared with simulation of Gnedin (2000).

## References

Anderson, S. F., et al. 2001, AJ, 122, 503
Becker, R. H., et al. 2001, AJ, 122, 2850
Boyle, B. J., et al. 2000, MNRAS, 317, 1014
Fan, X. 1999, AJ, 117, 2528
Fan, X., et al. 2000, AJ, 120, 1167
Fan, X., et al. 2001a, AJ, 121, 54
Fan, X., et al. 2001b, AJ, 122, 2833
Fan, X., et al. 2002, AJ, 123, 1247
Fan, X., et al. 2003, AJ, 125, 1649
Geballe, T., et al. 2002, ApJ, 564, 466
Gnedin, N. 2000, ApJ, 535, 530
Gunn, J. E., et al. 1998, 116, 3040
Gunn, J. E., & Peterson, B. A. 1965, ApJ, 142, 1633
Haiman, Z., & Loeb, A., 1998, ApJ, 503, 505
Hamman, F., & Ferland, G. 1993, ApJ, 418, 11
Hamman, F., & Ferland, G. 1999, ARA&A, 37, 487
Knapp, G. R., et al. 2004, in preparation
Leggett, S. K., et al. 2002, ApJ, 564, 452
Pentericci, L., et al. 2002, AJ, 123, 2151
Richards, G. T., et al. 2001, AJ, 121, 2308

Schmidt, M., Schneider, D. P., & Gunn, J. E. 1995, ApJ, 110, 68
York, D. G., et al. 2000, AJ, 120, 1579